

Characterization and Hydrothermal Conversion of Lignin Produced from Corncob Acid Hydrolysis Residue

Chao Wang, Gaojin Lyu,* Guihua Yang,* Jiachuan Chen, and Weikun Jiang

Lignin is one of the main components of corncob acid hydrolysis residue (CAHR). It can be used as a feedstock for biomaterial and biochemical production *via* biorefining. In this study, CAHR lignin was extracted, and enzymatic/mild acidolysis lignin (EMAL) was produced to ensure efficient lignin recovery. Next, hydrothermal conversion of the EMAL was carried out. The influences of process conditions including the temperature, time, and mass ratio of deionized water to EMAL on the hydrothermal conversion were thoroughly investigated to quantify analysis of the aromatics. EMAL produced from CAHR had a structure of the G-S-H type, in which the p-hydroxyphenyl unit was the primary structural unit, followed by the guaiacyl structural unit. The syringyl structural unit was less common. The yields (wt. %) of phenol, guaiacol, and 4-ethyl-phenol reached maxima of 1.26%, 0.75%, and 1.16%, respectively, at a reaction temperature of 310 °C and time of 30 min with a mass ratio of 80:1.

Keywords: Corncob acid hydrolysis residue; Enzymatic/mild acidolysis lignin; Hydrothermal conversion; Phenolic compounds

Contact information: Key Lab of Pulp and Paper Science & Technology of Ministry of Education, Qilu University of Technology, Jinan, Shandong, PR China, 250353;

* *Corresponding authors:* gaojinlv@qlu.edu.cn; ygh2626@126.com

INTRODUCTION

With the development of industry and an increasing demand for energy, fossil fuels such as natural gas, coal, and petroleum (Sobrino *et al.* 2010) remain the world's primary energy source. Fossil fuels are the feedstock for producing useful chemicals. However, fossil materials are non-renewable, and their exhaustion is inevitable. Therefore, green biofuels produced from lignocellulosic materials and agricultural wastes, such as bio-ethanol and bio-butanol, are receiving worldwide attention (Bozell 2010). Corncobs, a ubiquitous agricultural waste, are the main feedstock for ethanol and xylitol production *via* acid hydrolysis. The main by-product of these reactions, corncob acid hydrolysis residue (CAHR), is produced from the corncob-to-xylitol pretreatment process. Lignin is one of the main components of CAHR (Dizhbite *et al.* 2011). Recovery of lignin from the CAHR will yield a valuable co-product from agricultural wastes and allow for the effective use of lignin that otherwise goes to waste. The separation of lignin from CAHR in an economical fashion is a promising research opportunity that could give initiative for the construction of biorefineries.

Lignin consists of phenylpropane units substituted by zero, one, or two methoxyl groups. These structural building blocks of lignin are joined together by ether linkages (C-O-C) and carbon-carbon bonds (C-C). The most common type of lignin monomer is the β -O-4 structure. A number of studies have been undertaken regarding the liquefaction of lignin (Hoekman *et al.* 2011; Kleinert and Barth 2008; Pandey and Kim 2011; Yang *et al.*

2013). Lignin is an attractive potential raw material for the production of valuable chemicals. Research teams have used various organic solvents and ionic liquids as reaction media. Gosselink *et al.* (2011) converted organosolv hardwood and wheat straw lignin to a phenolic oil consisting of oligomeric fragments and monomeric aromatic compounds. The reaction medium they used was a supercritical fluid consisting of carbon dioxide, acetone, and water (temperature, 300 to 370 °C; pressure, 100 bar). They achieved a total yield of 10 to 12% based on the mass of lignin. Cheng *et al.* (2012) showed that a supercritical mixture of water and ethanol (50/50, v/v) was more effective than pure ethanol in depolymerizing alkali lignin. Cox and Ekerdt (2012) successfully depolymerized oak wood lignin in an acidic ionic liquid, 1-H-3-methylimidazolium chloride, under mild conditions (110 to 150 °C). However, the hydrothermal conversion behavior of lignin from CAHR has rarely been reported. Therefore, research in liquefaction of residue lignin, the main component of CAHR, is of potential value and practical importance for further and better understanding of hydrothermal conversion behavior of the CAHR.

In this study, the hydrothermal conversion behavior of lignin produced from CAHR was thoroughly investigated. CAHR lignin was first extracted to produce enzymatic/mild acidolysis lignin (EMAL). This step was done to ensure the lignin was efficiently recovered. Next, it was analyzed by an element analyzer, a Fourier transform infrared spectrometer (FT-IR), and a nuclear magnetic resonance spectrometer (NMR) to characterize its structure. Finally, hydrothermal conversion of the EMAL was carried out and the degraded compounds were identified and quantified by gas chromatography mass spectrometry (GC/MS). Process conditions of the hydrothermal conversion, including temperature, time, and mass ratio of deionized water to EMAL, were varied to quantify analysis of the aromatics.

EXPERIMENTAL

Materials

Corncob was obtained from Shandong province, China. CAHR was collected from a continuous acid hydrolysis process used to convert corncob to xylitol. Before extraction, the pH of the deionized water containing the residues was 6.5. The CAHR was washed with deionized water to remove residual soil and was then air-dried at room temperature. The moisture content of the CAHR was determined to be 4.6% *via* oven-drying at 105 °C to a constant weight. The cellulose, hemicellulose, and lignin contents of the CAHR were determined according to TAPPI standards (TAPPI 1975; TAPPI 1988; TAPPI 1999). The contents (w/w) of the CAHR were as follows: holocellulose, 63.52%; lignin, 18.39%; and hemicellulose, 6.00%, on a dry basis.

Throughout all experiments, all chemicals were of reagent grade and were used without further purification.

EMAL Extraction, Isolation, and Purification

The raw materials were ground in a Wiley mill and screened in the range of 40- to 60-mesh sizes (0.28 to 0.45 mm). The experimental samples were then ball-milled by a Hitachi ball-mill for 120 h. Before isolation, the CAHR were first washed with a mixture of benzene and ethanol (2/1, v/v) for 8 h to remove extractives and then dried in a vacuum oven at 50 °C. The requisite enzymatic/mild acidolysis lignin (EMAL) was obtained using a modified enzymatic/mild acidolysis method previously reported (Wu *et al.* 2006; Lou

and Wu 2011). Generally, two important steps are included in EMAL process: (1) cellulose enzymatic hydrolysis, and (2) mild acidolysis. It was further purified by n-hexane. The yield of EMAL recovered from CAHR was 54.8% (wt% of lignin in dry CAHR).

Analysis

The contents of carbon (C), hydrogen (H), nitrogen (N), and sulfur (S) in CAHR and EMAL were determined by a CHNS/O analyzer (Vario EL III, Elementar Analysensysteme, Germany). The oxygen contents of CAHR and EMAL were calculated by subtracting the C, H, N, and S contents from 100%.

EMAL (1 mg) and 300 mg of potassium bromide (KBr) were mixed and ground. An appropriate amount of the mixture was added to the tablet press sample grooves to obtain a thin, transparent tablet to be analyzed by FT-IR spectroscopy (IR Prestige-21, Shimadzu, Japan). FTIR spectra were recorded in the wave number range of 400 to 4000 cm^{-1} with a resolution of 0.5 cm^{-1} .

The bonds and functional groups of EMAL were analyzed with an NMR spectrometer (Bruker AVANCE II 400 MHz) equipped with a Quad probe dedicated to ^{31}P , ^{13}C , ^{19}F , ^{15}N , and ^1H acquisition at 35 °C. The NMR apparatus used an inverse gated decoupling pulse sequence. ^{13}C NMR was carried out by dissolving approximately 170 mg of EMAL in 1.8 mL of dimethyl sulfoxide- d_6 (DMSO- d_6). A sweep width of 10000 Hz was observed and spectra were accumulated with a time delay of 12 s between pulses. The presence of aliphatic hydroxyl groups, phenolic hydroxyl groups, and carboxyl functional groups in the EMAL were quantitatively determined using ^{31}P NMR spectra (Crestini and Argyropoulos 1997).

Hydrothermal Conversion in Subcritical Water

EMAL experimental samples were dried at 105 °C for 24 h. The hydrothermal conversion of EMAL was carried out in a 200-mL Hastelloy autoclave reactor (ZNHW-1, Zhengxin instrument plant, China) equipped with a pressure gauge. The reactor was heated to the required temperature (250 to 340 °C) at a heating rate of 10 °C/min. The time spent at the required temperature was varied from 0 to 60 min. The mass ratios of deionized water to EMAL tested were 60:1, 80:1, 100:1, and 120:1 (w/w).

EMAL (1 g) was mixed with deionized water at the required ratio in the reactor. The reactor was sealed and purged with high-purity nitrogen for three purging-vacuum evacuation cycles. It was then heated to the required temperature and was held at that temperature for the required time. The reactor was rapidly cooled to room temperature in an ice-water bath when the reaction ended. The mixture of liquids and solids from the reaction was washed with ethyl acetate and collected. The solids and liquids were separated using vacuum filtration with filter paper and a G-3 filter. The liquefied products of EMAL extracted into the ethyl acetate were put into a separating funnel to assist in the separation of the organic and aqueous phases. The conversion of EMAL was calculated according to the following equation,

$$\text{EMAL Conversion (wt. \%)} = \left(\frac{m_{\text{EMAL}} - m_i}{m_{\text{EMAL}}} \right) \quad (1)$$

where m_i is the mass of the hydrothermal residue and m_{EMAL} is the mass of the EMAL used for the reaction.

Characterization of Products Derived from EMAL

The chemical contents of the liquefied products were determined by GC/MS (QP2010, Shimadzu, Japan). A REX-5MS capillary column (30 m × 0.25 mm × 0.25 μm) was used, with helium gas as the carrier at a split ratio of 20:1 for the GC/MS analysis. The chemical components of the phenolic compounds and vanillin were identified and quantified using the internal standard method. Naphthalene was used as the internal standard. In a typical iteration of GC/MS testing, 1 μL of liquid containing naphthalene was injected into the GC and the GC separation program was run under the following conditions: injection temperature, 230 °C; initial oven temperature, 50 °C; 5 °C/min heating to 160 °C; and finally, 10 °C/min heating to 250 °C. Identification of compounds was performed by comparing the mass spectra (MS) data to data in National Institute of Standards and Technology (NIST) library.

The solid residues were analyzed by elemental analysis and FT-IR.

RESULTS AND DISCUSSION

Components of the CAHR and EMAL

The results of the elemental analyses of the CAHR and EMAL (based on dry weight) are shown in Table 1. The results showed that the empirical formula of CAHR could be expressed as $(C_{10}H_{12.86}O_{9.02}N_{0.07}S_{0.06})_n$. It was composed of carbon (42.83%), hydrogen (4.623%), oxygen (51.459%), nitrogen (0.347%), and sulfur (0.741%). The empirical formula of EMAL could be expressed as $(C_{10}H_{10.58}O_{4.46}N_{0.12}S_{0.03})_n$, and its components were carbon (58.69%), hydrogen (5.213%), oxygen (34.847%), nitrogen (0.789%), and sulfur (0.461%).

Table 1. Elemental Components of CAHR and EMAL (wt. %)

	C	H	O ^a	N	S
CAHR	42.83	4.62	51.46	0.35	0.74
EMAL	58.69	5.21	34.85	0.79	0.46

a: Calculated as difference

The FTIR spectra of CAHR and EMAL are presented in Fig. 1. The typical bands are listed in Table 2. Peaks in Fig.1 were assigned according to the literature (Faix 1991). Figure 1 shows wide absorption bands at a wave number of 3430 cm^{-1} (see Table 2, number 1), which were caused by the O-H stretching vibration of hydroxyl groups. This peak represents a typical functional group of lignin (Huang *et al.* 2012). The weak absorption bands (see Table 2, number 2) at 2930 cm^{-1} and 1380 cm^{-1} signify the existence of alkyl groups within the sample. The absorption band at 1707 cm^{-1} (see Table 2, number 3) is the characteristic absorption peak of the O-H group of aldehydes and ketones. The absorption band at 1707 cm^{-1} indicates that the C=O bands were not related to the aromatic rings. The absorption peaks at 1460 and 1600 cm^{-1} show that EMAL had aromatic rings. According to the absorption peaks shown in Fig. 1 and Table 2, the benzene ring skeleton stretching vibrations were indicative of strong absorption, meaning that the ring structure was well-protected. The characteristic absorption peaks of saturated aromatic hydrocarbons and aromatic C-H groups were considered to be within the range of 1400 to 1300 cm^{-1} and at 833 cm^{-1} . Absorption peaks related to the syringyl groups showed strong absorption, which

indicated syringyl groups were present in the lignin. The band at 1128 cm^{-1} is a better signal of a G-S lignin (Faix 1991). Furthermore, the additional band at 1163 cm^{-1} is typical for G-S-H lignin.

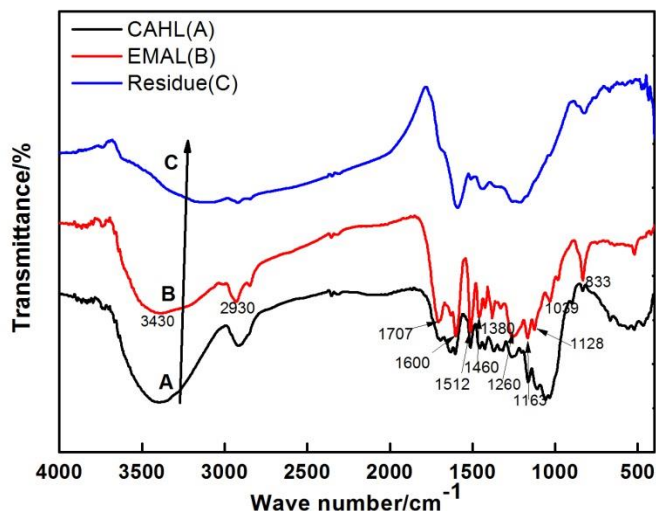


Fig. 1. FTIR spectra of CAHR, EMAL, and hydrothermal conversion residue (treatment at $340\text{ }^{\circ}\text{C}$, for 30 min, with an 80:1 water-to-EMAL ratio)

Table 2. FT-IR Analysis of CAHR, EMAL, and Hydrothermal Conversion Residue

Number	Wavenumbers (cm^{-1})	Assignment (bond)
1	3430	O-H stretching vibration
2	1380, 2930	C-H stretching vibration
3	1707	C=O stretching vibration
4	1460, 1600	Aromatic ring C=C stretching vibration
5	1512	Aromatic ring skeleton vibration
6	1423	CH_3 deformation vibration of alkane
7	1260	Guaiacyl ring breathing with C-O stretching
8	1163	Aliphatic ether C-O-H asymmetric vibration
9	1128	C-H in plane deformation vibration of syringyl units
10	1039	Aromatic ring C-H in plane bending vibration
11	833	C-H stretching vibration of syringyl units

As shown in Fig. 2 and Table 3, different β -O-4 linkages (55.0 to 62.0 ppm and 66.0 to 60.0 ppm) were important features of the structural units of EMAL. In addition, some other linkages (β - β , β -5, and 5-5) had significant carbon atom absorption peaks (52.0 to 54.0 ppm and 63.5 ppm). Further, the signal was weak in the range of 90.0 to 100.0 ppm, indicating that degradation of carbohydrates linked to lignin was thorough in the moderately severe acid hydrolysis stage. Data obtained from the ^{13}C NMR spectra of EMAL confirm the purity of the lignin. At the same time, the ^{13}C NMR characterizations show that EMAL was similar to typical lignin, with a G-S-H structure.

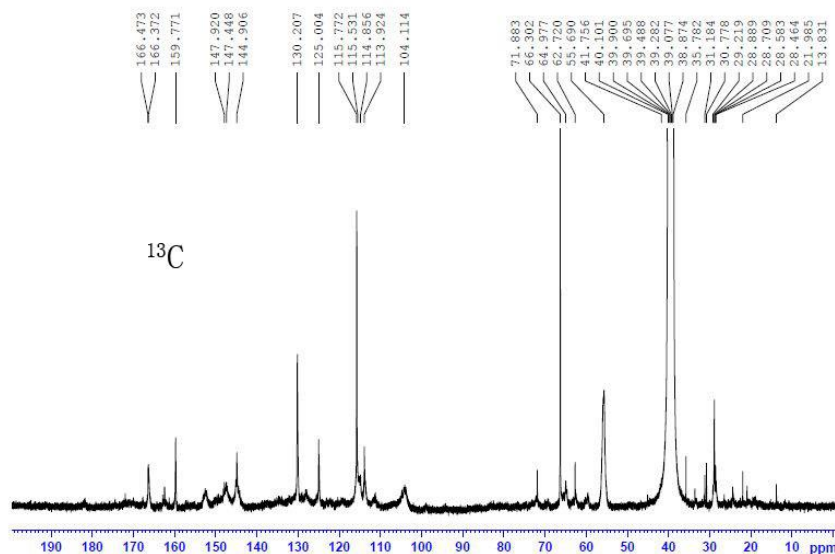


Fig. 2. ^{13}C NMR spectra of EMAL from CAHR

Table 3. Characteristics of the Structure and Functional Groups in EMAL as determined from ^{13}C NMR Spectra

Number	Chemical shift (ppm)	Characteristics of the structure and functional groups
1	0 to 35.0	C in saturated aliphatic chain
2	47.0 to 52.0	Isotaxiresinol type structures
3	52.0 to 54.0	C_β in β - β + β -5 structures
4	55.0 to 57.0	Methoxyl groups
5	59.0 to 60.9	C_γ in β -O-4 structures without $\text{C}_\alpha=\text{O}$
6	61.0 to 62.0	C_γ in cinnamyl alcohol structures
7	62.5 to 66.0	C_γ in β -O-4 structures with $\text{C}_\alpha=\text{O}$
8	90.0 to 100.0	Linkage band With LCC
9	100 to 123	C-H
10	123 to 126	C-C
11	137 to 156	C-O
12	160 to 162	C_4 in H units
13	163 to 168	$\text{C}_\alpha=\text{O}$ in COOH and CH-COOH

The ^{31}P -NMR spectra of EMAL samples in Fig. 3 show that some primary aliphatic hydroxyl groups, phenolic hydroxyl groups, and carboxyl functional groups existed within the lignin. The signal areas associated with these hydroxyl groups can be obtained. According to the amount of the internal standard detected, the content of each functional group was calculated (in mmol/g), and results are listed in Table 4. The aliphatic hydroxyl group content was 3.857 mmol/g and the phenolic hydroxyl group content was 4.410 mmol/g. The p-hydroxy-phenyl OH group content was 2.027 mmol/g, which accounts for 45.96% of the total phenolic hydroxyl groups. The increased content of p-hydroxy-phenyl OH groups confirmed that the EMAL from the corncob was of the G-S-H type. Thus, the EMAL had a G-S-H structure in which the p-hydroxyphenyl structural unit was the most prevalent, followed by the guaiacyl structure unit. The syringyl structure unit was the least common.

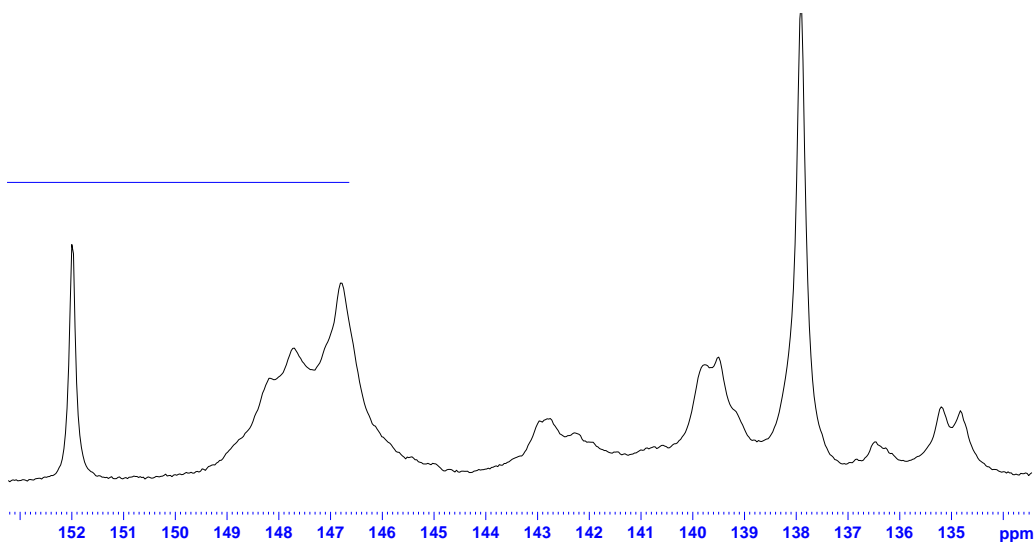


Fig. 3. ^{31}P NMR spectra of EMAL from CAHR

Table 4. Signals of Functional Groups of EMAL from CAHR

Functional group	Chemical shift (ppm)	Content of functional group (mmol/g)
Aliphatic OH group	149.2 to 146.0	3.857
Guaiacyl OH (G-OH)	140.0 to 138.8	1.436
p-hydroxy-phenyl OH (H-OH)	138.2 to 137.4	2.027
Syringyl OH (S-OH)	143.1 to 142.38	0.947
Total phenolic OH	-	4.410
Unknown phenolic OH	-	0.346
Total condensed type phenolic OH	144.5 to 143.1	0.154
	142.38 to 141.5	0.074
Total content of OH group	-	8.841
Carboxylic acids	135.5 to 134.5	0.777

Hydrothermal Conversion of EMAL

There are generally three fractions that result from the hydrothermal conversion process of EMAL, of which the liquid product is the main topic of research. The liquid phase can be further separated into an aqueous phase and an organic phase. The liquid products in the two phases were notably different. Generally, the major liquid products of EMAL produced from the hydrothermal conversion process were in the organic phase (Toor *et al.* 2011).

The conversion yield of EMAL in a hydrothermal conversion process is dependent on the reaction temperature, time, and the ratio of deionized water to EMAL. The temperature is the most important parameter affecting conversion yield, whereas time has the highest impact on the formation of lignin degradation products, such as aliphatic hydroxyls, phenolic hydroxyls, and carboxyl groups.

Effect of temperature on hydrothermal conversion

The effect of temperature on EMAL conversion is shown in Fig. 4A. The experiment was carried out at a water-to-EMAL ratio of 80:1 for 30 min. As can be seen in Fig. 4A, the conversion yield of EMAL increased with increasing temperature. A high yield (86%) of EMAL conversion was obtained when the temperature increased to 280 °C. Furthermore, the yield of the liquid product was about 95% at 340 °C. Some other studies

have obtained the same results regarding the hydrothermal degradation of cornstalk lignin (Ye *et al.* 2012).

Effects of time on hydrothermal conversion

The effect of time on EMAL conversion is shown in Fig. 4B. These experiments were carried out at 280 °C, with a water-to-EMAL ratio of 80:1, for 0 to 60 min. Figure 4B illustrates that the conversion yield reached a maximum of 78% when after 10 min of reaction. However, the conversion yield decreased with increasing the time from 10 min onward, under the conditions tested. Some previous studies have shown that when the reaction time is longer at high temperature and pressure, some products can undergo repolymerization or crosslinking reactions with the alcoholic groups and phenolic rings of the lignin-degradation intermediates (Yuan *et al.* 2010; Jin *et al.* 2011; Cheng *et al.* 2012). Therefore, the optimal time for EMAL conversion was determined to be 10 min.

Effects of the mass ratio on hydrothermal conversion

The effect of the ratio of deionized water to EMAL on the conversion yield of the hydrothermal conversion process run at 310 °C for 30 min is shown in Fig. 4C. The conversion yield of EMAL increased slightly with increasing mass ratio, and all conversion yields at different ratios were in the range of 90 to 94%. The ratio of water to EMAL therefore had less impact on the conversion of EMAL than the other parameters tested.

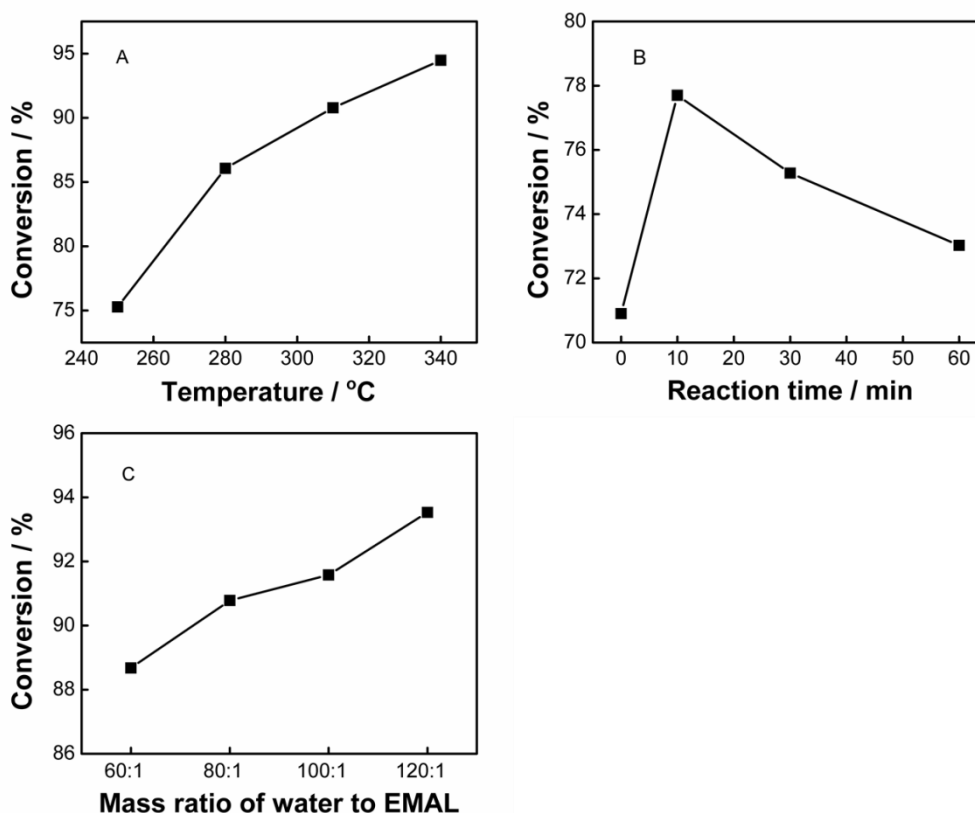


Fig. 4. Conversion behavior of EMAL with varying temperature (A), reaction time (B), and mass ratio of water to EMAL (C)

GC/MS Analysis

The results of the qualitative and quantitative GC/MS analyses of the organic fractions of EMAL produced from the hydrothermal conversion process are shown in Table 5. GC/MS spectra of the liquid products obtained under different conditions showed fewer compounds. This implies that the depolymerized product at subcritical conditions was composed mostly of nonvolatile, large molecules. This result was similar to what another study previously reported (Cheng *et al.* 2012).

In this study, it was found that the yield of conversion products was low under subcritical conditions (less than 2%, on a 1-g dry EMAL basis). The results in Table 5 show that the phenolic compounds included phenol, 4-methyl-phenol, guaiacol, 4-ethyl-phenol, and vanillin. When the experiment was carried out at a mass ratio of 80:1 for 30 min, the yield of liquid products increased with increasing reaction temperature, but some of the main phenolic compounds reached maximum yield at 310 °C. The yields of the phenol, guaiacol, and 4-ethyl-phenol reached maxima of 1.26%, 0.75%, and 1.16% (on a dry EMAL basis), respectively, at 310 °C with a mass ratio of 80:1 and a 30 min reaction time. Decomposition of EMAL can be achieved even under subcritical conditions; cleavage of C-O-C bonds (*e.g.*, β -O-4) occurred in subcritical water at high enough temperatures. In particular, various phenols and methoxyl phenols were formed as basic products. According to ¹³C NMR analysis, some small-molecule compounds (phenol, 4-ethylphenol, and 2,3-dihydrobenzofurane) originated from the H-type structural unit of lignin, while other small-molecule compounds (guaiacol and 2,6-dimethoxy-phenol) originated from G- and S-type structural units.

Table 5. Composition of Liquid Fractions Obtained from EMAL Hydrothermal Conversion

RT	Compound	EMAL hydrothermal conversion in the following condition									
		T (°C), t (min), m (100%)									
		250 ^a	280 ^a	310 ^a	340 ^a	0 ^b	10 ^b	60 ^b	60:1 ^c	100:1 ^c	120:1 ^c
5.35	Ethyl benzene	0	0	0.09	0	0	0	0	0	0	0.05
5.14	1,2-dimethyl-benzene	0	0	0	0	0	0	0	0.09	0	0
7.8	Phenol	0.16	0.44	1.26	1.02	0.1	0.11	0.25	0.73	0.063	0.74
10.95	4-methyl-phenol	0	0	0.05	0.11	0	0	0	0	0	0.03
11.06	guaiacol	0.23	0.32	0.75	0.62	0.1	0.12	0.17	0.44	0.36	0.43
13.36	4-ethyl-phenol	0.1	0.38	1.16	0.98	0.1	0.13	0.21	0.92	0.75	0.89
13.94	Naphthalene(Internal standard)	1.01	1.01	1.01	0.96	1	0.93	1.01	0.93	0.94	0.94
14.04	2-methoxy-4-methyl-phenol	0	0	0.06	0.09	0	0	0	0.05	0.04	0.04
14.89	2,3-dihydro-benzofuran	0.06	0.11	0	0	0.2	0.17	0.08	0	0	0
16.35	4-ethyl-2-methoxy-phenol	0.02	1.09	0.29	0.24	0	0	0.04	0	0.16	0.22
16.94	1-methyl-naphthalene	0.09	0	0.08	0	0.1	0.16	0.06	0.21	0.2	0.16
17.4	2-Naphthaleneacetic acid	0	0	0	0	0	0	0	0.09	0	0
17.43	4-ethenyl-2-methoxy-phenol	0.06	0	0	0	0.2	0.17	0.11	0.05	0	0
18.22	2,6-dimethoxy-phenol	0.03	0.2	0.27	0.21	0	0	0.06	0	0.15	0.19
19.08	2-ethenyl-naphthalene	0.32	0.95	0.21	0.24	0.2	0.34	0.17	0.21	0.19	0.17
19.43	Vanillin	0.08	0.07	0.05	0	0.13	0.10	0.09	0.08	0.09	0.09
19.57	Vanillic acid	0	0	0	0	0	0	0	0	0.03	0
20.01	2,7-dimethyl-naphthalene	0	0.1	0	0	0.1	0.08	0.04	0.04	0	0
26.43	4-Hydroxy-3,5-dimethoxy-benzaldehyde	0	0	0.05	0.79	0	0	0	0.04	0.04	0.05

a: 30 min, 80:1 mass ratio; b: 250 °C, 80:1 mass ratio; c: 310 °C, 30 min

Solid Residues

The hydrothermal conversion residue was black like char when experiments were performed in subcritical water. In subcritical water, the yield of insoluble product was high at 250 °C (about 25%). However, the yield decreased with increasing conversion temperature. The yield of insoluble product increased when the conversion time was 30 min. Some studies (Wahyudiono *et al.* 2008; Pińkowska *et al.* 2012) have shown that lower-molecular-weight, soluble compounds form polymers and cross-link with phenolic biochar. Repolymerization *via* radical coupling and carbonization *via* recondensation reactions were promoted with increases in temperature.

The composition of the solid residues obtained at 250 °C with a mass ratio of 80:1 and 30 min cooking time correspond to the typical composition of EMAL. With an increase in reaction temperature to 340 °C, some changes in the elemental composition of the solid residue occurred. The respective empirical formula $[C_{10}H_{5.62}O_{1.85}N_{0.10}S_{0.07}]_n$ was significantly different from that of the EMAL subjected to hydrothermal conversion in subcritical water.

The FT-IR spectrum in Fig. 5A resembled the spectrum in Fig. 5B, which indicates that the structure and functional groups were probably the same. However, some differences were observed in the 1200 to 650 cm^{-1} region: the vibrations of ether bonds and aromatic rings disappeared in Fig. 5B. The typical band of O-H group stretching vibrations disappeared from the range of 3600 to 3000 cm^{-1} , which confirms the loss of phenolic and alcoholic groups (Pińkowska *et al.* 2012; Wahyudiono *et al.* 2008).

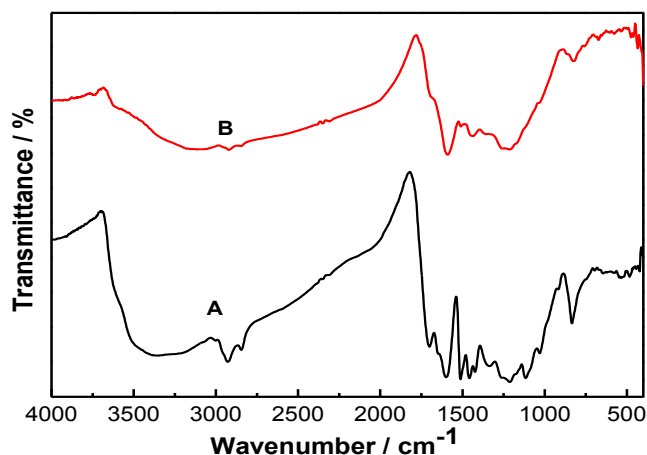


Fig. 5. FTIR spectra of the EMAL hydrothermal conversion residue;
A: temperature of 250 °C, reaction time of 30 min, water-to-EMAL ratio of 80:1;
B: temperature of 340 °C, reaction time of 30 min, water-to-EMAL ratio of 80:1

CONCLUSIONS

1. EMAL from corncob acid hydrolysis residue had a structure of the G-S-H type, in which the p-hydroxyphenyl structural unit was the primary structural unit, followed by the guaiacyl structural unit. The syringyl structural unit was less common.
2. EMAL can be converted into useful resources by hydrothermal decomposition in subcritical water. Many compounds were quantified. The yields (wt. %) of phenol,

guaiacol, and 4-ethyl-phenol reached maxima of 1.26%, 0.75%, and 1.16%, respectively (on the basis of dry EMAL) when the reaction took place at 310 °C, with a mass ratio of 80:1, for 30 min.

3. Decomposition of EMAL can be achieved even under subcritical conditions. Cleavage of C-O-C bonds (e.g., β -O-4) occurred in subcritical water at high temperatures. Small-molecule compounds, e.g. phenol, 4-ethylphenol, and 2,3-dihydrobenzofuran, came from the H-type structural unit of the lignin. Small-molecule compounds such as 2-methoxy-phenol and 2,6-dimethoxy-phenol came from the G- and S-type structural units of the lignin.

ACKNOWLEDGEMENTS

The authors are grateful for the financial support from the National Science Foundation of China (Grant Nos. 31170547, 31270627, 31370580, 31270626), the Natural Science Foundation of Shandong Province (Grant Nos. ZR2010CM065, ZR2011CM011), the Outstanding Young Scientist Award Fund of Shandong province (BS2013NJ014), and the Director Fund of KLPPST (No. 08031334).

REFERENCES CITED

- Bozell, J. J. (2010). "Connecting biomass and petroleum processing with a chemical bridge," *Science* 329(5991), 522-523.
- Cheng, S. N., Wilks, C., Yuan, Z. S., Leitch, M., and Xu, C. B. (2012). "Hydrothermal degradation of alkali lignin to bio-phenolic compounds in sub/supercritical ethanol and water-ethanol co-solvent," *Polym. Degrad. Stab.* 97(6), 839-848.
- Cox, B. J., and Ekerdt, J. G. (2012). "Depolymerization of oak wood lignin under mild conditions using the acidic ionic liquid 1-H-3-methylimidazolium chloride as both solvent and catalyst," *Bioresour. Technol.* 118, 584-588.
- Crestini, C., and Argyropoulos, D. S. (1997). "Structural analysis of wheat straw lignin by quantitative ³¹P and 2D NMR spectroscopy. The occurrence of ester bonds and α -O-4 substructures," *J. Agric. Food Chem.*, 45(4), 1212-1219.
- Dizhbite, T., Telysheva, G., Dobele, G., Arshanitsa, A., Bikovens, O., Andersone, A., and Kampars, V. (2011). "Py-GC/MS for characterization of non-hydrolyzed residues from bioethanol production from softwood," *J. Anal. Appl. Pyrolysis.* 90(2), 126-132.
- Faix, O. (1991). "Classification of lignins from different botanical origins by FT-IR spectroscopy," *Holzforschung*, 45(s1), 21-28.
- Gosselink, R. J., Teunissen, W., Van Dam, J. E., Jong, E. D., Gellerstedt, G., Scott, E. L., and Sanders, J. P. (2011). "Lignin depolymerisation in supercritical carbon dioxide/acetone/water fluid for the production of aromatic chemicals," *Bioresour. Technol.* 106 (1), 173-177.
- Hoekman, S. K., Broch, A., and Robbins, C. (2011). "Hydrothermal carbonization (HTC) of lignocellulosic biomass," *Energy Fuels* 25(4), 1802-1810.
- Huang, Y. Q., Wei, Z. G., Qiu, Z. J., Yin, X. L., and Wu, C. Z. (2012). "Study on structure and pyrolysis behavior of lignin derived from corncob acid hydrolysis residue," *J. Anal. Appl. Pyrolysis.* 93(1), 153-159.

- Jin, Y., Ruan, X., Cheng, X., and Lü, Q. (2011). "Liquefaction of lignin by polyethyleneglycol and glycerol," *Bioresour. Technol.* 102(3), 3581-3583.
- Kleinert, M., and Barth, T. (2008). "Towards a lignin-cellulosic biorefinery: Direct one-step conversion of lignin to hydrogen-enriched biofuel," *Energy Fuels* 22(2), 1371-1379.
- Lou, R., and Wu, S. B. (2011). "Products properties from fast pyrolysis of enzymatic/mild acidolysis lignin," *Appl. Energy* 88(1), 316-322.
- Pandey, M. P., and Kim, C. S. (2011). "Lignin depolymerization and conversion: A review of thermochemical methods," *Chem. Eng. Technol.* 34(1), 29-41.
- Pińkowska, H., Wolak, P., and Złocińska, A. (2012). "Hydrothermal decomposition of alkali lignin in sub- and supercritical water," *Chem. Eng. J.* 187(1), 410-414.
- Sobrinho, F. H., Monroy, C. R., and Pérez, J. L. H. (2010). "Critical analysis on hydrogen as an alternative to fossil fuels and biofuels for vehicles in Europe," *Renew. Sust. Energ. Rev.* 14(2), 772-780.
- TAPPI (1975). "Holocellulose in wood," TAPPI Standard Test Method T9wd-75.
- TAPPI (1988). "Acid-insoluble lignin in wood and pulp," TAPPI Standard Test Method T222om-88.
- TAPPI (1999). "Alpha-, beta-, and gamma-cellulose in pulp," TAPPI Standard Test Method, T203cm-99.
- Toor, S. S., Rosendahl, L., and Rudolf, A. (2011). "Hydrothermal liquefaction of biomass: A review of subcritical water technologies," *Energy* 36(5), 2328-2342.
- Wahyudiono, Sasaki, M., and Goto, M. (2008). "Recovery of phenolic compounds through the decomposition of lignin in near and supercritical water," *Chem. Eng. Process.* 47(9), 1609-1619.
- Wu, S. B., Guo, Y. L., Wang, S. G., and Li, M. S. (2006). "Chemical structures and thermochemical properties of bagasse lignin," *Forestry Studies in China* 8(3), 34-37.
- Yang, G. H., Jahan, M. S., and Ni, Y. H. (2013). "Structural characterization of pre-hydrolysis liquor lignin and its comparison with other technical lignins," *Curr. Org. Chem.* 17(15), 1589-1595.
- Ye, Y. Y., Fan, J., and Chang, J. (2012). "Effect of reaction conditions on hydrothermal degradation of cornstalk lignin," *J. Anal. Appl. Pyrolysis.* 94(1), 190-195.
- Yuan, Z., Cheng, S., Leitch, M., and Xu, C. (2010). "Hydrolytic de-polymerization of alkaline lignin in hot-compressed water and ethanol," *Bioresour. Technol.* 101(23), 9308-9313.

Article submitted: January 16, 2014; Peer review completed: May 12, 2014; Revised version received and accepted: June 10, 2014; Published: June 17, 2014.